applied sciences

MDPI

Article

The Effect of Synthesis Procedure on Hydrogen Peroxidase-Like Catalytic Activity of Iron Oxide Magnetic Particles

Atripan Mukherjee [1,2], Amir M. Ashrafi [1,2], Pavel Svec [1], Lukáš Richtera [1,2,*], Jan Přibyl [3], Martin Brtnický [4,5,6], Jindrich Kynicky [7] and Vojtěch Adam [1,2]

1 Department of Chemistry and Biochemistry, Mendel University in Brno, Zemedelska 1, CZ-613 00 Brno, Czech Republic; xmukherj@mendelu.cz (A.M.); amirmansoor.ashrafi@mendelu.cz (A.M.A.); pavel.svec@mendelu.cz (P.S.); vojtech.adam@mendelu.cz (V.A.)
2 Central European Institute of Technology, Brno University of Technology, Purkynova 123, CZ-612 00 Brno, Czech Republic
3 European Institute of Technology, Masaryk University, Kamenice 753/5, CZ-625 00 Brno, Czech Republic; jan.pribyl@ceitec.muni.cz
4 Department of Geology and Pedology, Faculty of Forestry and Wood Technology, Mendel University in Brno, Zemedelska 3, CZ-613 00 Brno, Czech Republic; martin.brtnicky@mendelu.cz
5 Department of Agrochemistry, Soil Science, Microbiology and Plant Nutrition, Faculty of AgriSciences, Mendel University in Brno, Zemedelska1, CZ-613 00 Brno, Czech Republic
6 Institute of Chemistry and Technology of Environmental Protection, Faculty of Chemistry, Brno University of Technology, Purkynova 118, CZ-621 00 Brno, Czech Republic
7 BIC Brno, spol. s r.o., Purkyňova 648/125, CZ-612 00 Brno, Czech Republic; kynicky@bicbrno.cz
* Correspondence: lukas.richtera@mendelu.cz; Tel.: +42-054-513-3311; Fax: +42-054-521-2044

Received: 17 July 2020; Accepted: 22 September 2020; Published: 27 September 2020

Abstract: A comparative study was carried out using magnetic nanoparticles (MNPs) for the fabrication of non-enzymatic sensors for the continuous and rapid detection and monitoring of H_2O_2. Various MNPs, differing in terms of their synthesis procedure and modification, were synthesized and characterized by different techniques. The electrochemical catalytic activity of the synthesized MNPs toward the reduction in H_2O_2 was investigated by cyclic voltammetry. The naked MNPs showed the highest catalytic activity among all the synthesized MNPs. The biosensor based on the naked MNPs was then applied in the determination of H_2O_2 using chronoamperometry. The parameters such as the applied cathodic potential and the amount of MNPs on the developed biosensor were optimized. Moreover, the analytical figures of merit, including reproducibility (RSD = 6.14%), sensitivity (m = 0.0676 μA μM^{-1}), limit of detection (LOD) = 27.02 μmol L^{-1}, and limit of quantification (LOQ) = 89.26 μmol L^{-1} of the developed biosensor indicate satisfactory analysis. Finally, MNPs were successfully utilized for the determination of H_2O_2 in milk.

Keywords: magnetic nanoparticle; nanozyme; chronoamperometry; biosensor; peroxidase-like activity

1. Introduction

In the field of analytical biology, various biomolecules have significant molecular information encoded with dynamic and spontaneous coordinates following different biochemical processes. Most of them are naturally electro-inactive and required to transduce through a receptor to form an electroactive compound [1]. Therefore, secondary byproducts like H_2O_2 are important biological messengers that are considered as significant biomarkers for the *in vivo* and *in vitro* detection of complex biomolecules [2]. This simple molecule, H_2O_2, belongs to the classes of reactive oxygen species (ROS), compounds with

significance in the field of clinical and diagnostics, food manufacturing, environmental field [3,4]. The pathological and physiological importance of H_2O_2 is associated with signal transduction, apoptosis, and cell activation [5,6]. Because of their antibacterial properties, they are sometimes used in the food and packaging industry [7]. The Food and Drug Administration (FDA) recommended the maximum treatment level for using H_2O_2 in different types of food and beverages [8]. Moreover, the extensive use of H_2O_2 in food packaging and processing is harmful to health. Acting as an adulterant, it can cause severe gastrointestinal problems [9]. Hence, early and continuous monitoring with the effective detection of H_2O_2 is important for the pharmaceutical sector and the food industry, as well as clinical and diagnostics application sectors [10–13]. In the recent past, continuous, online and real-time monitoring of analytes were significant in order to study, control, and investigate them in different environmental conditions. Conventional methods like spectrophotometric, chemiluminescent, fluorometric methods are used for H_2O_2 detection and quantification [14–16]. Expensive reagents, skilled technicians and extended analysis times are the common drawbacks of these conventional methods, while continuous and online monitoring have extended their applications.

Biosensors are expected to be highly specific, selective and sensitive towards their target analytes, along with possessing online-monitoring features [17,18]. Electrochemical biosensors are applied for effective continuous monitoring and detection of complex biomolecules [19]. Moreover, amperometric methods can detect and continuously measure kinetic information in real time [20,21]. Electrochemical biosensors based on enzymes are well studied and widely used for the detection of different species. However, the inherent properties of enzymes such as degradability, and being unstable in severe conditions of pH and temperature, have limited the application of enzyme-based sensors. Furthermore, each enzyme catalyzes a specific reaction at an optimum pH. When the pH of the medium is far from the optimum pH of the enzyme, its catalytic activity decreases substantially.

Nanozymes (NEs) are defined as the catalytic nanomaterials that mimic natural enzymes catalytic activity. Compared to their natural analogs, NEs are advantageous in terms of their higher stability, lower cost, resistance to external influences, simple synthesis, long-term storage, and size/composition-dependent activity. Accordingly, due to their unique properties, NEs attract the researcher's attention to apply them in different areas such as biosensing [22]. Moreover, as nanoscale materials, NEs have a sufficiently large area that is useful in the conjugation of multiple ligands for biorecognition [23]. Furthermore, their activity could be further modulated by different approaches, such as synthetic strategy, which means modification through the composition, size, and shape of the NEs [24].

Magnetic nanoparticles (MNPs) were reported to possess a peroxidase-like activity and were applied in biosensing devices [25,26]. The main aim of this study is to compare the sensitivity towards the reduction in H_2O_2 by MNPs synthesized by different synthetic strategies. The results will help to provide an insight into the effect of the synthesis approach on the enzymomimetic properties of MNPs.

2. Materials and Methods

Multi-walled carbon nanotubes (MWCNT), ferric chloride hexahydrate ($FeCl_3 \cdot 6H_2O$), iron chloride tetrahydrate ($FeCl_2 \cdot 4H_2O$), chitosan with medium molecular weight (deacetylated chitin), tetraethylorthosilicate (TEOS), ammonium solution (28.0–30.0% NH_3 basis), N, N-dimethylformamide (DMF), sodium chloride (NaCl), potassium chloride (KCl), sodium phosphate dibasic (Na_2HPO_4), ascorbic acid, potassium dihydrogen phosphate (KH_2PO_4), hydrogen peroxide solution (30% in H_2O, contains stabilizer), and Nafion® 117 solutions (5% in a mixture of lower aliphatic alcohol and water) were purchased from Sigma-Aldrich (St. Louis, MO, USA). Absolute ethanol was purchased from VWR (Radnor, PA, USA). The glassy carbon electrode (GCE), (d = 3 mm) was purchased from the BASi (West Lafayette, IN, USA). The water (18.20 MΩ cm) used for solution preparation was first double-distilled by an Aqua Osmotic 02 (Aqua Osmotic, Tisnov, Czech Republic) and then deionized by using a Millipore RG (Milli-Q water, Millipore Corp., Billerica, MA, USA). Autolab electrochemical

analyzer model 2.1 software (Metrohm Autolab, Utrecht, The Netherland) was used for running the electrochemical experiments.

Phosphate-buffered saline (PBS; 0.01 M) was used in the electrochemical measurements. A solution of 0.1 M hydrogen peroxide (H_2O_2) was freshly prepared as a stock solution and used for the analysis. Nafion (NF; 1%) was prepared by neutralization of NF using an 8.0% ammonium solution.

A three-electrode configuration was used for the electrochemical measurements, where a platinum electrode was used as a counter electrode, Ag/AgCl (1.0 M, KCl) as the reference electrode and a modified GCE served as a working electrode.

2.1. Preparation of MWCNT Dispersion

MWCNT (2.0 mg) was dispersed in 1 mL of DMF and sonicated for 40 min to get a homogenous dispersion. The desired volume of the prepared dispersion was dropped on the cleaned GCE and dry-casted at room temperature.

2.1.1. Synthesis of Naked Iron Oxide Magnetic Nanoparticles (UN-MNPs)

Magnetic particles were synthesized, after being inspired from a previous study, using $FeCl_3{\cdot}6H_2O$ and $FeCl_2{\cdot}4H_2O$ as precursor materials, then modified accordingly [27]. A volume of 50 mL of 0.32 M $FeCl_3{\cdot}6H_2O$ was mixed with 50 mL of 0.2 M $FeCl_2{\cdot}4H_2O$ using a magnetic stirrer at 600 RPM for 2 h. A volume of 50 mL of the mixture was then injected into a flask containing 100 mL of Milli-Q water and heated for 90 °C. At 50 °C, a volume of 30 mL of undiluted ammonium solution was added and heated up to 90 °C for 1 h by using a four-propeller mechanical stirrer at 300 RPM. The MNPs were washed by magnetic separation five times using 200 mL of Milli-Q water. The formation of MNPs were confirmed using a magnetic bar during washing with magnetic separation.

2.1.2. Synthesis of Chitosan Modified Iron Oxide Magnetic Nanoparticles (MNPs-CH)

Chitosan-modified MNPs (MNPs-CH) were synthesized by mixing 50 mL of $FeCl_3{\cdot}6H_2O$ 0.32 M and 50 mL of $FeCl_2{\cdot}4H_2O$ 0.2 M using a magnetic stirrer at 600 RPM for 2 h. The mixture was transferred and allowed to be heated under constant stirring using a mechanical rotor at 300 RPM. At 40 °C, 0.25 mg of chitosan was added into the mixture under heating conditions. At 50 °C, 30 mL of undiluted ammonium solution was added as a reducing agent and heated up to 90 °C for 1 h. [27]. The MNPs-CH were washed threefold using 70% ethanol and Milli-Q water, respectively. The formation of MNPs-CH was confirmed by using a magnetic bar.

2.1.3. Synthesis of MNPs Modified with TEOS (MNPs-TEOS)

Following the previous method, naked MNPs (UN-MNPs) were synthesized and subsequent modification with TEOS was carried out according to a previous study [28]. UN-MNPs were thoroughly cleaned and dispersed in Milli-Q water followed by 5 min of sonication. Absolute ethanol was added and sonicated for another 5 min followed by the addition of 8 mL of undiluted ammonium solution. The mixture was subjected to mechanical stirring at 300 RPM with the addition of 0.5 mL TEOS for 3 h. The magnetic separation procedure was used for washing the obtained particles. The obtained particles were washed threefold by using 70% ethanol, followed by washing with Milli-Q water, respectively.

2.2. Preparation of the Working Electrode

The bare GCE was polished with a polishing pad using diamond suspension (0.5 μm) for 2 min followed by sonication in Milli-Q water and absolute ethanol for 9 min, respectively. The cleaning procedure was continued by polishing the electrode with different alumina slurries of 1.0 μm, 0.3 μm, 0.05 μm, followed by washing after each cleaning step with Milli-Q water and absolute alcohol for 9 min, respectively. The GCE was modified by using 10 μL of well-dispersed MWCNT in DMF and was then allowed to air-dry. The electrode was further modified by using 10 μL of different types

of synthesized MNPs and allowed to air-dry. NF (1%; 5 μL) was added to the modified electrode to protect the immobilized materials from being washed away.

2.3. Characterization of MNPs

The Synthesized unmodified and modified MNPs were characterized by using SEM and energy-dispersive X-Ray Spectroscopy-SEM (EDX)The different samples of MNPs were attached to the stub and subjected to SEM imaging. Images of samples were made on a MIRA 3 SEM from the TESCAN company (TESCAN Ltd., Brno, Czech Republic, EU). The used detectors have In-Beam secondary electrons (SE) with an accelerating voltage of 15 kV. The working distance was set to 3 mm and ultra-high resolution was used as a scan mode. The measurement was performed in a high vacuum. Elemental analysis was done on the energy-dispersive x-ray spectroscopy (EDX) detector X-MAX 50 (Oxford instruments plc, Abingdon, UK) with high vacuum conditions and an accelerating voltage of 15 kV. A silicon composite stub was used for the elemental analysis of UN-MNPs and MNPs-CH, whereas an aluminum composite stub was used for the MNPs-TEOS. The working distance was 15 mm and an external SE detector was used. The input energy for the UN-MNPs was set to 20,000–25,000 cts, the output energy was set to about 10,000–11,000 cts, and dead time fluctuated between 50–54%. The input energy for the modified MNPs was set to 11,000–13,000 cts, the output energy was set to about 7700–8500 cts, and dead time fluctuated between 30–36%. The time for each analysis was 20 min, whereas the spot size was approximately 75 nm. The concentration of Fe in the synthesized MNPs was determined by atomic absorption spectroscopy (AAS) 280Z AA (Agilent Technologies, Santa Clara, CA, USA) with electrothermal atomization, using Zeeman background correction. Moreover, inductively coupled plasma mass spectroscopy (ICP-MS) (Agilent Technologies, Tokyo, Japan), was also applied for the determination of concentrations.

2.4. Cyclic Voltammetry

The electrochemical behavior of the prepared sensors using different MNPs was studied in presence of H_2O_2 by cyclic voltammetry (CV). The CV parameters are as follows: start potential 0.0 V, stop potential 0.0 V, scan rate 50 mV s^{-1}, upper vertex potential 1.0 V, and lower vertex potential −1.0 V. The potential was scanned towards the anodic direction.

2.5. Chronoamperometry and Optimization

For amperometric measurements, a desired potential magnitude was applied on the working electrode and the resulting currents that followed between the counter and working electrodes were sampled every 1 s with a 3000-s measurement duration.

2.6. Repeatability

The repeatability of the modified sensors was investigated by using the same electrode for successive injections of the analyte. Moreover, the repeatability was evaluated by using the same electrode consecutively for amperometric measurements under the same conditions. The sensitivity of each study was compared to evaluate the stability of the sensors.

2.7. Selectivity

Potential interfering agents were selected to study the selectivity of the sensors towards H_2O_2. The selected interfering agents were NaCl, KCl, glucose, and ascorbic acid with a uniform stock concentration of 0.1 M, respectively. The amount of interfering agents upon injection in the electrochemical cell was 100 μmol L^{-1}, which was equal to that of the analyte.

2.8. Real Sample Analysis

The accuracy of the prepared sensor was tested by calculating the recovery rate of H_2O_2 spiked in a milk sample. A milk sample containing 3.9% of fat was purchased from the local market. Unboiled milk (90 µL) was mixed with 10 µL of 0.1 M H_2O_2. Then, the as-prepared sample (100 µL) was injected into the electrochemical cell containing electrolytes (10 mL PBS) followed by threefold standard injections of 100 µmol L^{-1} of H_2O_2. The same electrode was used thrice to obtain the average recovery.

3. Results and Discussion

3.1. Characterization of MNPs

The different synthesized unmodified and modified MNPs were characterized by SEM and EDX–SEM techniques (Figure 1). The chemical composition of different MNPs is clearly shown in Figure 1, where the presence of the oxygen in the proximity of the iron confirms the successful synthesis of the iron oxide magnetic particles. Iron and oxygen are present in all the MNPs. The elemental analysis table for the presence of Fe, O, and other element compositions are represented in S1, S2 and S3 in the Supplementary Materials. A silicon composite stub was used for the UN-MNPs and MNPs-CH, whereas an aluminum composite stub was used for the mapping of MNPS-TEOS, respectively. The homogenous dispersion of the selected MNPs on the MWCNT/GCE can be observed in Figure 1D. From the image, the rod-like structure belongs to the MWCNT, whereas drop-cast MNPs can be seen, in the sphere-like structure, to from GCE/MWNT/UN-MNPs. The MNPs were further characterized by using an energy-dispersive X-ray fluorescence (ED-XRF) spectrometer (S4, S5 and S6 in the Supplementary Materials). The characterization of the MNPs by ED-XRF confirms the presence of Fe in all the synthesized particles, while silicon only exists in MNP-TEOS. Moreover, Fourier-transformed infrared spectroscopy (FTIR-ATR) spectra (S7 in the Supplementary Materials), and Raman spectroscopy (S8 in the Supplementary Materials) were done to confirm the modification of MNPs by chitosan and TEOS. The modified particles show the presence of Si-O and O-H in their IR spectra appearing at the same wavenumber as TEOS and chitosan, respectively. Moreover, the Fe-O bond appears in all the synthesized particles. The Fe-O bond also appears in the Raman spectra of the synthesized particles. Transmission electron microscopy (TEM) was done to confirm the particle size and dispersion (S9–S12 in the Supplementary Materials). As can be seen, the UN-MNPs are spheric particles with a uniform size smaller than 50 nm. On the other hand, MNP-CH contains the particles which are far from the spheric shape and have an altered uniform size distribution. MNP-TEOS particles are more aggregated. Furthermore, the size of the different synthesized MNPs was studied by dynamic light scattering (DLS) (S13 in the Supplementary Materials), where all the particles show almost the same average size, even though multi-dispersity in MNP-TEOS is visible. The Fe content in different MNPs was studied by using AAS and ICP-MS, respectively (S14 and S15 in the Supplementary Materials). The Fe density of the UN-MNPs was found to be almost identical to both AAS and ICP-MS, which can indicate that these particles form a stable dispersion. The concentration of MNP-CH is almost the same as UN-MNP. However, the concentration of MNP-TEOS dispersion is several times higher, which might be due to the existence of high aggregation and, consequently, more concentrated dispersion. The different synthesized MNPs were found to be less than 50 nm, as characterized by TEM. Moreover, from SEM, and confirmed by TEM, it was observed that the synthesized MNPs were accumulating and found to be present in the cluster. This clustering was responsible for the larger size of MNPs, as observed in DLS. The working principle of DLS is Brownian motion and this was unable to identify individual nanoparticles from heavy clusters.

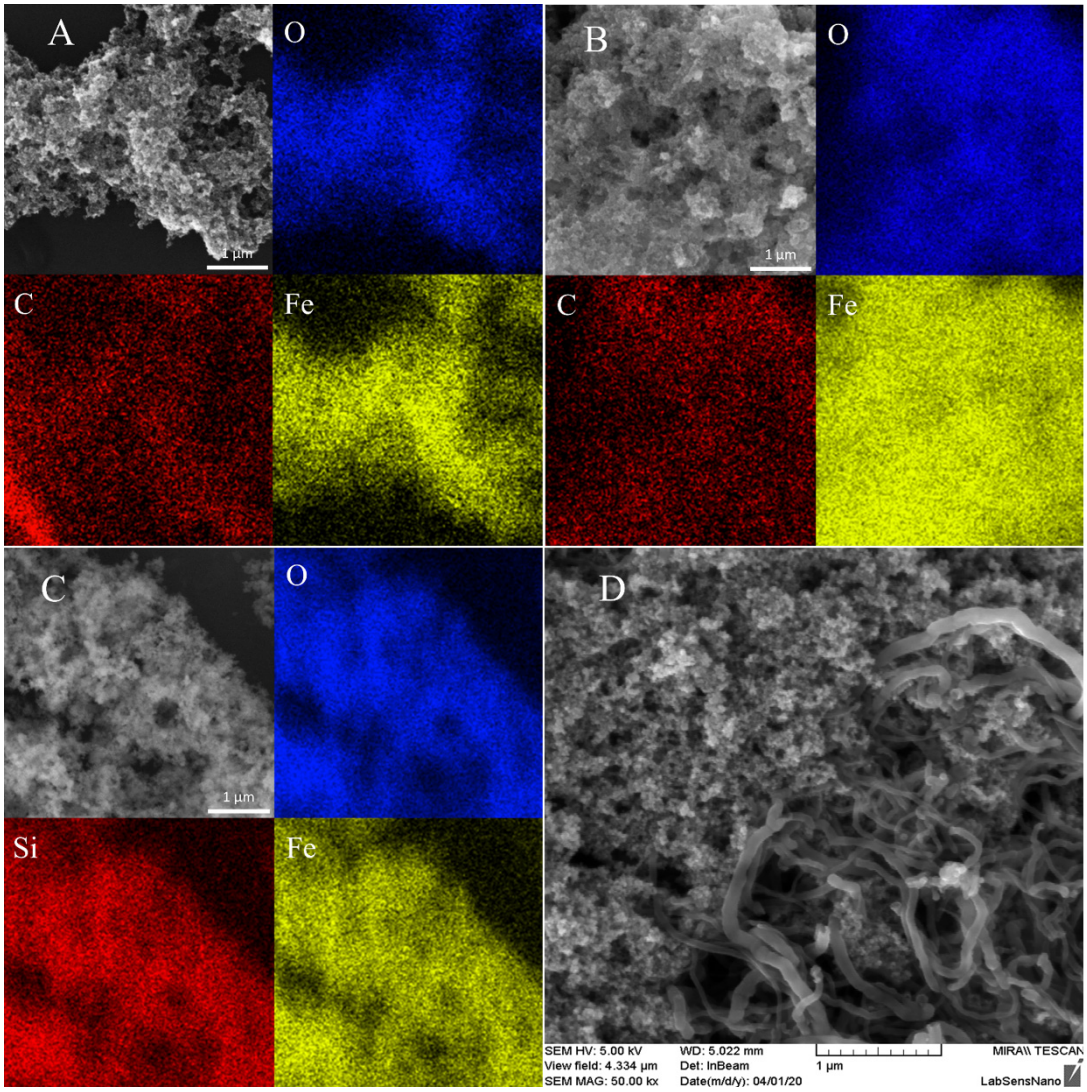

Figure 1. SEM image and elemental mapping images representing the constituent of (**A**) naked magnetic nanoparticles (UN-MNPs), (**B**) chitosan-modified MNPs (MNPs-CH), (**C**) MNPs modified with tetraethylorthosilicate (MNPs-TEOS); (**D**) SEM image representing the uniform distribution of UN-MNPs drop-cast on glassy carbon electrode (GCE)/multi-walled carbon nanotubes (MWCNT) to form GCE/MWCNT/UN-MNPs.

3.2. Electrochemical Behavior of the Modified Electrode

The electrochemical behavior of the developed electrodes is represented in Figure 2. As seen in Figure 2A, the modified electrode with MWCNT, GCE/MWCNT, brought about a broad cathodic current in the presence of H_2O_2 starting from −0.3 V. An increase in the cathodic current was observed with GCE/MWCNT/MNPs-CH upon the addition of H_2O_2, starting from −0.5 V in Figure 2B. No change in the current was observed with the addition of H_2O_2 in solution when GCE/MWCNT/MNPs-TEOS were used as the working electrode in Figure 2C. However, when GCE/MWCNT/UN-MNPs were utilized (Figure 2D), with the addition of H_2O_2, a high reduction peak appeared. Compared to GCE/MWCNT, the reduction in H_2O_2 starts at lower potential magnitudes (−0.2 V) in GCE/MWCNT/UN-MNPs. Thus, it can be concluded that the naked electrocatalytic activity of UN-MNPs toward a reduction in hydrogen peroxide is the highest. The reduction in H_2O_2 takes place by electron transfer from the electrode. Therefore, the UN-MNPs act as wires, which facilitate the electron transfer to H_2O_2. Overall, the peroxidase-like activity of the UN-MNPs stems from their electron transfer ability by reducing

substrates and H_2O_2. Based on the obtained results, it can be concluded that the MNPs that were exposed directly to H_2O_2 possess a higher electrocatalytic effect.

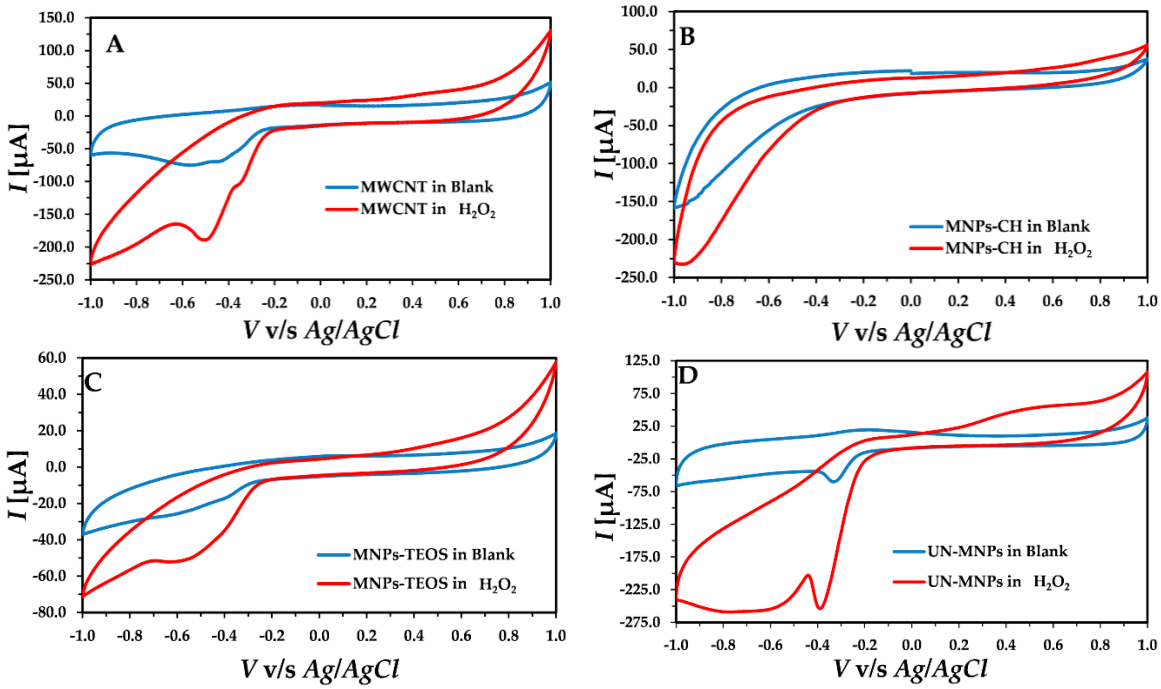

Figure 2. Cyclic voltammetry (CV) recorded using different developed electrodes in the presence and absence of H_2O_2: (**A**) CV of the GCE/MWCNT; (**B**) GCE/MWCNT/MNPs-CH. (**C**) GCE/MWCNT/MNPs-TEOS; (**D**) GCE/MWCNT/UN-MNPs.

3.3. Optimization of the Conditions

For online, rapid, and fast detection, the chronoamperometry method was selected. After analyzing the CV, UN-MNPs were selected due to their high electrocatalytic effect, resulting in higher sensitivity towards the H_2O_2 reduction compared to other modified MNPs. The reduction peak, as shown (Figure 2D), ranges from −0.1 V to −0.4 V. Hence, the applied potential in chronoamperometry varied in the range of −0.1 V to −0.4 V. The chronoamperometry was run with the stepwise addition of H_2O_2. By increasing the magnitude of the applied cathodic potential, the sensitivity of the calibration curve increased in Figure 3. To avoid the reduction in redox-active compounds, −0.3 V was selected as the applied potential, even though −0.4 V shows better sensitivity. It must be taken into account that a lower potential magnitude (−0.3 V) is favorable as it causes fewer interfering effects by other electroactive compounds present in the solution.

The number of UN-MNPs drop-cast on the MWCNT/GCE can improve the sensitivity of the proposed biosensor. GCE/MWCNT/UN-MNPs were prepared where the amount of drop-cast UN-MNPs was varied from 10 µL to 30 µL. The highest sensitivity was observed with only 10 µL of the UN-MNPs and a larger volume did not cause a higher sensitivity.

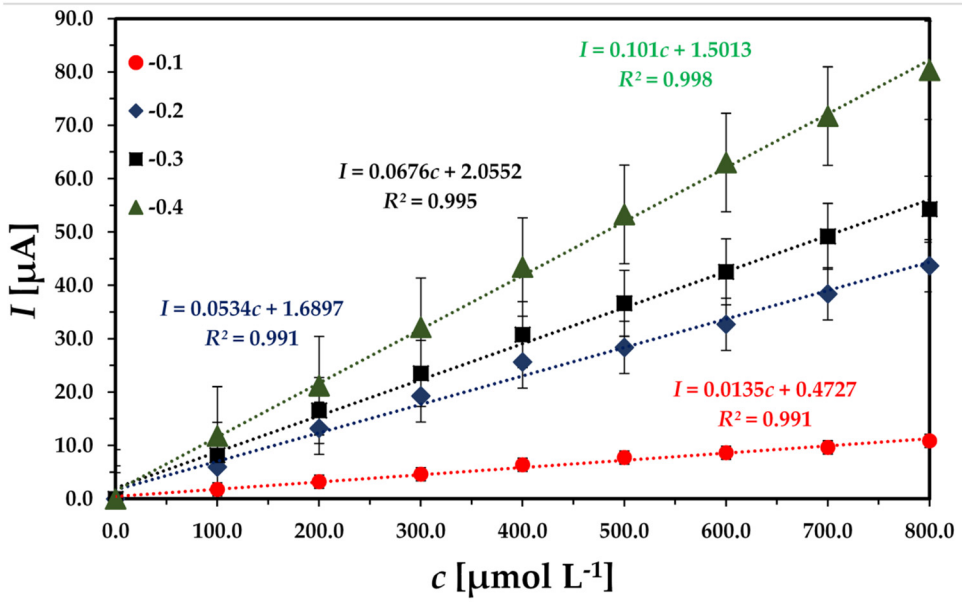

Figure 3. Comparing the sensitivity of the sensor at different applied potentials: 0.01 M phosphate-buffered saline (PBS), 7.4 pH with continuous injection of H_2O_2 containing 100 µmol L^{-1} in each injection.

3.4. Analytical Study

3.4.1. Linear Range Detection

The developed GCE/MWCNT/UN-MNPs were used to detect H_2O_2 at an applied potential of −0.3 V with a concentration range from 99.9 µmol L^{-1} to 792.86 µmol L^{-1}. The cathodic current response increased linearly with the consecutive injection of H_2O_2 (R^2= 0.995) in Figure 4. The slope of the calibration curve is regarded as the sensitivity of the electrode. The developed sensor had a sensitivity of 0.0676 µA μM^{-1}. The limit of detection (LOD) was calculated by using "3 s/m", where "s" is defined as the standard deviation of the current response and "m" is the slope of the calibration curve. The LOD was found to be 27.02 µmol L^{-1}. The limit of quantification (LOQ) was calculated as 89.26 µmol L^{-1} by using the formula "10 s/m" and is presented in Table 1.

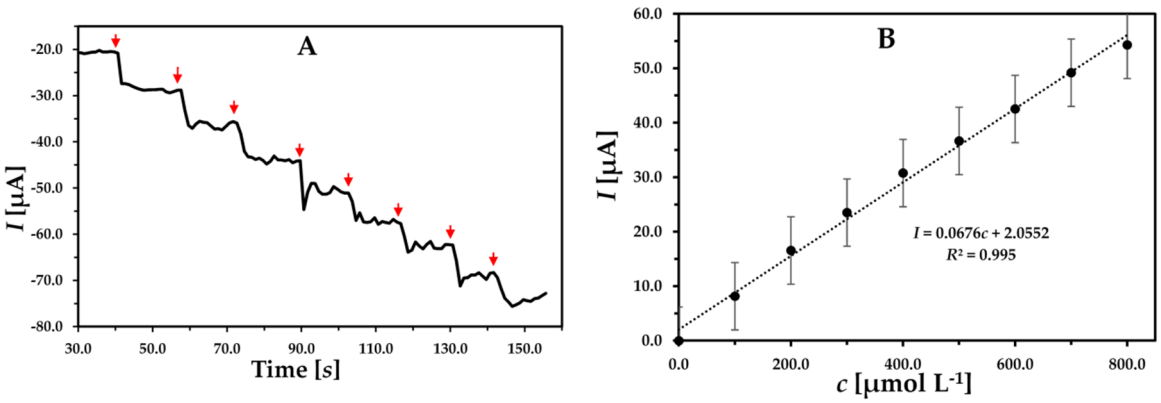

Figure 4. (**A**) Chronoamperogram and (**B**) related concentration dependence of peak current obtained using GCE/MWCNT/UN-MNPs. Successive injections of 100 µmol L^{-1} H_2O_2; applied potential of −0.3 V in 10 mL 0.01 M PBS buffer.

Table 1. Analytical parameters of the developed sensor GCE/MWCNT/UN-MNPs at an applied potential of −0.3 V for H_2O_2 detection.

Linear ranges	99.90–792.86 µmol L^{-1}
Slope	0.068 µA $µM^{-1}$
Intercept	2.055µA
Sensitivity	0.068 µA $µM^{-1}$
Limit of detection LOD	27.020 µmol L^{-1}
Limit of Quantification LOQ	89.26 µmol L^{-1}
Relative standard deviation RSD%	6.14

3.4.2. Repeatability

The repeatability of the electrode was determined by using the same modified electrode consecutively three times and plotting consecutive calibration curves for H_2O_2 by chronoamperometry. As shown in Figure 5, the slopes of the calibration curve are very close to each other, where $\overline{X}$ = 0.0446, s = 0.0027, and reproducibility (RSD)% = 6.14, indicating the good repeatability of the developed sensor.

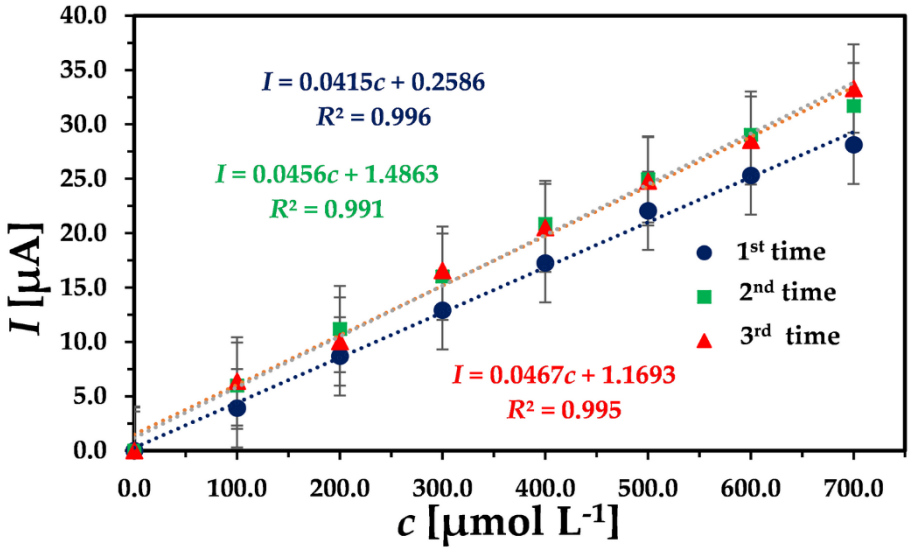

Figure 5. Three successive concentration dependencies of peak current obtained by chronoamperometry with the same GCE/MWCNT/UN-MNPs. Successive injection of 100 µmol L^{-1} H_2O_2 with an applied potential of −0.3 V in 10 mL 0.01 M PBS buffer.

3.4.3. Selectivity

The developed biosensor is intended to work in complex environments like the blood, body fluid, food samples, etc. Hence, the analytical performance of the developed biosensor should be studied to check the selectivity towards its analyte in the presence of potential and common interfering agents found in biological environments. The potential interfering agents for H_2O_2 detection was selected from previous study which are KCl, NaCl, glucose, and ascorbic acid [29]. The same concentration of the analyte and the interfering agents was used to study the selectivity and effect of the potential interfering agents. The measuring solution was subjected to successive double injections of 100 µmol L^{-1} of H_2O_2 standard, followed by injection with the same concentration of NaCl, KCl, glucose, ascorbic acid and, again, double injections of H_2O_2 at 100 µmol L^{-1}. As shown in Figure 6A, with each injection of H_2O_2, an apparent current drop was achieved, while no significant current response was observed with the addition of the potential interfering agents. With the last injections of H_2O_2, again, the current drop was realized by confirming the high selectivity of the developed sensor. The change in the current response with the addition of the interfering agent is also represented in Figure 6B.

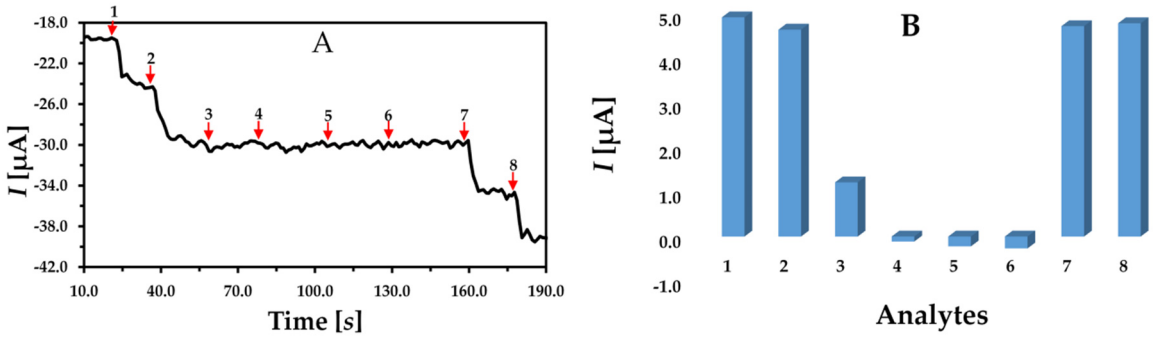

Figure 6. (**A**) Effect of the interfering compounds on the analytical response of the GCE/MWCNT/UN-MNPs using chronoamperometry. (**B**) The obtained current responses (1, 2, 7, and 8) denote injections of H_2O_2, while 3, 4, 5 and 6 denote NaCl, KCl, glucose and ascorbic acid, respectively. The applied potential was −0.3 V, and the concentration of all the injected agents was 100 µmol L^{-1}.

3.4.4. Real Sample Analysis

The practical application of the developed sensor was evaluated by the detection of H_2O_2 in milk without any pretreatment. To eliminate the matrix effect, the standard addition method was used with selected GCE/MWCNT/UN-MNP sensors at optimized conditions. At first, a volume of 100 µL of a prepared mixture of milk sample containing 90 µL of milk +10 µL of 0.1 M H_2O_2 was added into an electrochemical cell containing 10 mL of electrolyte followed by successive threefold standard additions of 100 µmol L^{-1} of H_2O_2 (10 µL injections). The obtained amperometric results are shown in Figure 7. This measurement was repeated thrice and the obtained results are presented in Table 2. The developed sensor has good sensitivity for practical applications towards the detection of H_2O_2. As represented, the obtained concentration was 102.92 ± 1.92 µmol L^{-1} while the spiked concentration was only 100 µmol L^{-1}). The fabricated sensor was able to recover H_2O_2 successfully with a recovery rate of 102.92%, which indicates high accuracy of the developed sensor [30].

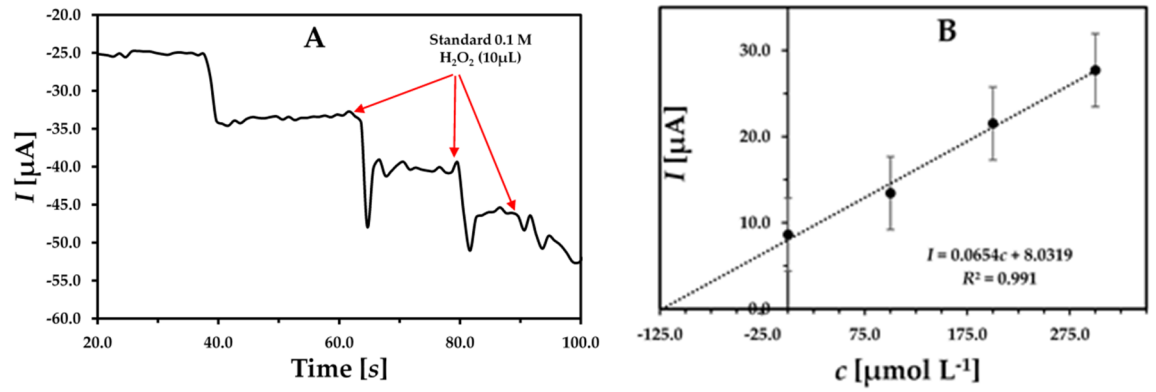

Figure 7. (**A**) The prepared milk sample analysis using multiple standard additions method with selected GCE/MWCNT/UN-MNP biosensors at −0.3 V. (**B**) The calibrated results of the spiked sample.

Table 2. Determination of H_2O_2 in milk sampled using GCE/MWCNT/UN-MNPs.

Spiked (µmol L^{-1})	Slope	Intercept	Found (µmol L^{-1})	Recovery
100	0.0733	7.5301	102.73 ± 1.92 (n = 3)	102.92%

4. Conclusions

The results obtained in the current work show that the catalytic activity of the MNPs mainly relies on the exposure of the naked surface of the MNPs to the target substrate. Further modification of the

synthesized MNPs impaired the peroxidase-like activity. Furthermore, the developed sensor based on UN-MNPs was successfully applied for the selective and sensitive determination of H_2O_2 at low potential magnitude, which improved the selectivity of the developed senor. The accurate determination of H_2O_2 in a milk sample was realized using the developed biosensor. Therefore, it was demonstrated that MNPs can be a promising alternative for the detection of natural enzymes with peroxidase-like activity. Because of the low cost, high stability, and durability of nanozymes, the developed sensor is advantageous compared to the analogous enzyme-based sensors. The developed biosensor can be used for the preliminary and rapid determination of H_2O_2 in foodstuffs. It can be also applied for the online monitoring of H_2O_2 in a flow system because of its short response time.

Supplementary Materials: The following are available online at http://www.mdpi.com/2076-3417/10/19/6756/s1, S1–S15: The synthesized different magnetic nanoparticles (MNPs) were furthered characterised by using techniques as described.

Author Contributions: Conceptualization, A.M. and A.M.A.; methodology and synthesis of MNPs, A.M.; validation, A.M., A.M.A.; formal analysis, A.M. and A.M.A.; sample and electrode characterization, P.S. and M.B. and J.K.; authors of the manuscript, A.M. and A.M.A.; FTIR, L.R.; Raman spectra, J.P.; final correction, V.A. and L.R. All authors have read and agreed to the published version of the manuscript.

Funding: This research was financially supported by the Ministry of Education, Youth and Sports of the Czech Republic (MEYS CR) under the Czech Infrastructure for Integrative Structural Biology (CIISB) research infrastructure project LM2015043, which supported the Atomic force microscopy (AFM) measurements at Nanobiotechnology Core Facility, and by Central European Institute of Technology (CEITEC) 2020 (LQ1601). CIISB research infrastructure project LM2018127, funded by MEYS CR, is gratefully acknowledged for the financial support provided for the measurements carried out at the Cryo-Electron Microscopy and Tomography Core Facility.

Conflicts of Interest: The authors declare no conflict of interest.

References

1. Labib, M.; Sargent, E.H.; Kelley, S.O. Electrochemical Methods for the Analysis of Clinically Relevant Biomolecules. *Chem. Rev.* **2016**, *116*, 9001–9090. [CrossRef] [PubMed]
2. Stone, J.R.; Yang, S. Hydrogen Peroxide: A Signaling Messenger. *Antioxid. Redox Signal.* **2006**, *8*, 243–270. [CrossRef] [PubMed]
3. Tsiafoulis, C.G.; Trikalitis, P.N.; Prodromidis, M.I.; Prodromidis, M.I. Synthesis, characterization and performance of vanadium hexacyanoferrate as electrocatalyst of H2O2. *Electrochem. Commun.* **2005**, *7*, 1398–1404. [CrossRef]
4. Manjare, S.T.; Kim, Y.; Churchill, D.G. Selenium- and Tellurium-Containing Fluorescent Molecular Probes for the Detection of Biologically Important Analytes. *Acc. Chem. Res.* **2014**, *47*, 2985–2998. [CrossRef] [PubMed]
5. Geiszt, M.; Leto, T.L. The Nox Family of NAD(P)H Oxidases: Host Defense and Beyond. *J. Biol. Chem.* **2004**, *279*, 51715–51718. [CrossRef]
6. Giorgio, M.; Trinei, M.; Migliaccio, E.; Pelicci, P.G. Hydrogen peroxide: A metabolic by-product or a common mediator of ageing signals? *Nat. Rev. Mol. Cell Biol.* **2007**, *8*, 722–728. [CrossRef]
7. Hsu, C.-L.; Chang, K.-S.; Kuo, J.-C. Determination of hydrogen peroxide residues in aseptically packaged beverages using an amperometric sensor based on a palladium electrode. *Food Control* **2008**, *19*, 223–230. [CrossRef]
8. U.S. Food & Drug Administration, CFR-Code of Federal Regulations Title 21. Available online: https://www.accessdata.fda.gov/scripts/cdrh/cfdocs/cfCFR/CFRSearch.cfm?fr=184.1366 (accessed on 1 April 2019).
9. Watt, B.E.; Proudfoot, A.T.; Vale, J.A. Hydrogen Peroxide Poisoning. *Toxicol. Rev.* **2004**, *23*, 51–57. [CrossRef]
10. Lee, Y.-D.; Lim, C.-K.; Singh, A.; Koh, J.; Kim, J.; Kwon, I.C.; Kim, S. Dye/Peroxalate Aggregated Nanoparticles with Enhanced and Tunable Chemiluminescence for Biomedical Imaging of Hydrogen Peroxide. *ACS Nano* **2012**, *6*, 6759–6766. [CrossRef]
11. Luo, Y.; Liu, H.; Rui, Q.; Tian, Y. Detection of Extracellular H2O2Released from Human Liver Cancer Cells Based on TiO2 Nanoneedles with Enhanced Electron Transfer of Cytochromec. *Anal. Chem.* **2009**, *81*, 3035–3041. [CrossRef]
12. Shu, X.; Chen, Y.; Yuan, H.; Gao, S.; Xiao, D. H2O2 Sensor Based on the Room-Temperature Phosphorescence of Nano TiO2/SiO2 Composite. *Anal. Chem.* **2007**, *79*, 3695–3702. [CrossRef] [PubMed]

13. Lu, X.; Zhou, J.; Lu, W.; Liu, Q.; Li, J. Carbon nanofiber-based composites for the construction of mediator-free biosensors. *Biosens. Bioelectron.* **2008**, *23*, 1236–1243. [CrossRef] [PubMed]
14. Matsubara, C.; Kawamoto, N.; Takamura, K. Oxo[5, 10, 15, 20-tetra(4-pyridyl)porphyrinato]titanium(IV): An ultra-high sensitivity spectrophotometric reagent for hydrogen peroxide. *Analyst* **1992**, *117*, 1781. [CrossRef]
15. Zhang, L.-S.; Wong, G.T. Optimal conditions and sample storage for the determination of H2O2 in marine waters by the scopoletin-horseradish peroxidase fluorometric method. *Talanta* **1999**, *48*, 1031–1038. [CrossRef]
16. Hanaoka, S.; Lin, J.-M.; Yamada, M. Chemiluminescent flow sensor for H2O2 based on the decomposition of H2O2 catalyzed by cobalt(II)-ethanolamine complex immobilized on resin. *Anal. Chim. Acta* **2001**, *426*, 57–64. [CrossRef]
17. Songa, E.A.; Okonkwo, J.O. Recent approaches to improving selectivity and sensitivity of enzyme-based biosensors for organophosphorus pesticides: A review. *Talanta* **2016**, *155*, 289–304. [CrossRef]
18. Putzbach, W.; Ronkainen, N.J. Immobilization Techniques in the Fabrication of Nanomaterial-Based Electrochemical Biosensors: A Review. *Sensors* **2013**, *13*, 4811. [CrossRef]
19. Wang, Y.; Huang, J.; Zhang, C.; Wei, J.; Zhou, X. Determination of Hydrogen Peroxide in Rainwater by Using a Polyaniline Film and Platinum Particles Co-Modified Carbon Fiber Microelectrode. *Electroanalysis* **1998**, *10*, 776–778. [CrossRef]
20. Michael, D.J.; Wightman, R.M. Electrochemical monitoring of biogenic amine neurotransmission in real time. *J. Pharm. Biomed. Anal.* **1999**, *19*, 33–46. [CrossRef]
21. Boyne, M.S.; Silver, D.M.; Kaplan, J.; Saudek, C.D. Timing of changes in interstitial and venous blood glucose measured with a continuous subcutaneous glucose sensor. *Diabetes* **2003**, *52*, 2790–2794. [CrossRef]
22. Wang, Q.; Wei, H.; Zhang, Z.; Wang, E.; Dong, S. Nanozyme: An emerging alternative to natural enzyme for biosensing and immunoassay. *TrAC Trends Anal. Chem.* **2018**, *105*, 218–224. [CrossRef]
23. Tang, Z.; Wu, H.; Zhang, Y.; Li, Z.; Lin, Y. Enzyme-Mimic Activity of Ferric Nano-Core Residing in Ferritin and Its Biosensing Applications. *Anal. Chem.* **2011**, *83*, 8611–8616. [CrossRef] [PubMed]
24. Wei, H.; Wang, E. Nanomaterials with enzyme-like characteristics (nanozymes): Next-generation artificial enzymes. *Chem. Soc. Rev.* **2013**, *42*, 6060. [CrossRef] [PubMed]
25. Yu, F.; Huang, Y.; Cole, A.J.; Yang, V.C. The artificial peroxidase activity of magnetic iron oxide nanoparticles and its application to glucose detection. *Biomaterials* **2009**, *30*, 4716–4722. [CrossRef] [PubMed]
26. Sun, L.; Ding, Y.; Jiang, Y.; Liu, Q. Montmorillonite-loaded ceria nanocomposites with superior peroxidase-like activity for rapid colorimetric detection of H_2O_2. *Sens. Actuators B Chem.* **2017**, *239*, 848–856. [CrossRef]
27. Gregorio-Jauregui, K.M.; Pineda, M.G.; Rivera-Salinas, J.E.; Hurtado, G.; Saade, H.; Martinez, J.L.; Ilyina, A.; López, R.G. One-Step Method for Preparation of Magnetic Nanoparticles Coated with Chitosan. *J. Nanomater.* **2012**, *2012*, 1–8. [CrossRef]
28. Li, Y.-S.; Church, J.S.; Woodhead, A.L.; Moussa, F. Preparation and characterization of silica coated iron oxide magnetic nano-particles. *Spectrochim. Acta Part A Mol. Biomol. Spectrosc.* **2010**, *76*, 484–489. [CrossRef] [PubMed]
29. Mollarasouli, F.; Kurbanoglu, S.; Asadpour-Zeynali, K.; Ozkan, S.A. Non-enzymatic monitoring of hydrogen peroxide using novel nanosensor based on CoFe2O4@CdSeQD magnetic nanocomposite and rifampicin mediator. *Anal. Bioanal. Chem.* **2020**, 1–13. [CrossRef] [PubMed]
30. Ye, D.; Li, H.; Liang, G.; Luo, J.; Zhang, X.; Zhang, S.; Chen, H.; Kong, J. A three-dimensional hybrid of MnO2/graphene/carbon nanotubes based sensor for determination of hydrogen-peroxide in milk. *Electrochim. Acta* **2013**, *109*, 195–200. [CrossRef]